Interference Analysis in the LTE and NB-IoT Uplink Multiple Access with RF impairments

Gustavo J. González, Fernando H. Gregorio, and Juan Cousseau
CONICET-Department of Electrical and Computer Engineering, Universidad Nacional del Sur, Argentina

***Abstract*—Narrowband internet of things (NB-IoT) considers the connection of thousands of devices to a single LTE base station (BS). To make possible the coexistence with classic LTE user equipements (UE)s, the BS allocates several IoT UEs into special physical resource blocks (PRB)s. These special PRBs reduce the IoT transmitter complexity but make the LTE signal interfere with the IoT PRBs. IoT nodes are in general low-cost and therefore prone to suffer from RF impairments. The LTE interference and the RF impairments compromise the performance of IoT nodes. In this paper, we analyze the coexistence of LTE and IoT in the multiple access uplink, considering RF impairments. We analyze the use of guard bands to reduce the interference from LTE in IoT. Also, we evaluate the allowable carrier frequency offset (CFO) and I/Q imbalance levels that ensures a reasonable system performance.**

***Index Terms*—Narrowband internet of things (NB-IoT), LTE.**

I. Introduction

Internet of things (IoT) is a new paradigm that involves the interconnection of thousands of devices and home appliances, such as TVs, fridges, light sensors, actuators, mobile phones, etc., to form a massive network. The implementation of IoT has a myriad of new applications, ranging from health care and surveillance, to more modern concepts as smart buildings and smart cities [1].

The support of IoT devices is a great challenge for cellular networks, as they were originally designed for voice calls and high data rate transfers in human-oriented applications [2]. Therefore, the coexistence between conventional and IoT-oriented services is a problem to be solved. In applications like smart metering, IoT applications typically require low data rate and are delay tolerant. On the other hand, in automobile safety systems or in industry, the implementations have tight delay requirements. As a consequence, thousands of devices with very different characteristics can appear connected in a single cell. These requirements motivate the development of a flexible and scalable physical interface.

IoT nodes have severe constraints in terms of power consumption. In some cases, battery powered devices must operate over 10 years without battery charge [3]. Additionally, the node implementation must be low cost to make affordable applications with large number of nodes [4].

The 3rd Generation Partnership Project (3GPP) started the standarization of an air-interface for IoT, known as Narrow-Band IoT (NB-IoT) [5], [6]. NB-IoT considers the coexistence of IoT devices with LTE users equipments (UE)s, by using the same basic unit of resource allocation, i.e., both systems use the same physical resource blocks (PRB)s. The standard defines an access network oriented to serve a massive number of low throughput, moderated delay, and low cost devices. Three operation modes are defined: a) guard band operation, b) in-band operation, and c) stand-alone operation. In this work, we focus on the in-band mode [7].

Considering the standard $15\,\mathrm{kHz}$ subcarrier spacing, the PRB occupies a bandwidth of $180\,\mathrm{kHz}$. In conventional applications (LTE-A), multiple PRBs are allocated to a single user. However, in case NB-IoT nodes, the use of sub-PRB transmission is also considered. For the downlink, NB-IoT uses the same intercarrier spacing than LTE. On the other hand, in the uplink a single tone mode with an intercarrier spacing of $3.75\,\mathrm{kHz}$ is included [8]. This mode is used by low data-rate power-constrained nodes, since the single carrier modulation leads to an efficient RF implementation, due to the low peak-to-average power ratio transmission. Additionally, the reduced channel bandwidth requires a quarter of the sampling frequency, and it allows the allocation of 48 IoT UEs in the same PRB [9].

In the base station, it is possible to use a common analog front-end to demodulate LTE and single tone IoT signals. However, the difference in the PRB structure destroys the orthogonality and creates interference. This situation affects the coexistence of LTE and NB-IoT users and needs to be carefully studied. Up to the authors knowledge, this important issue was not addressed in the literature. Moreover, the low cost constraint in IoT devices, creates several RF impairments that degrade the system performance. The coexistence between LTE and IoT devices is studied in this work. It is considered the interference produced not only by different structure of LTE and IoT PRBs but also by the most harmful RF impairments. We analyze the required bandwidth to obtain and adequate isolation between LTE and IoT systems. Additionally, we determine the allowable level of CFO and I/Q imbalance that the IoT uplink can tolerate without compromising the performance.

II. Signal Model

We analyze the scenario of a base station (BS) serving several LTE and IoT user equipments (UE)s at the same time. The base station (BS) allocates resource blocks (PRB)s to different LTE or IoT devices according to the network load.

For the downlink, IoT nodes use LTE numerology, i.e., $1/T_L$ $=15\,\mathrm{kHz}$ subcarrier spacing and a subframe of $1\,\mathrm{ms}$ formed by two slots of 7 OFDM symbols. An LTE PRB is formed by $M_L = 12$ contiguous subcarriers, during a slot.

As in the OFDMA case, there is no intercarrier or interuser interference in the downlink given that the BS is a time and frequency reference for different UEs. On the other hand, there are three possibilities for the IoT uplink: multitone transmission based on SC-FDMA with 15 kHz of intercarrier spacing, single-tone also with 15 kHz, and single tone with $1/T_I$ =3.75 kHz. In the 3.75 kHz single tone mode, the PRB M_I has 48 subcarriers (or different IoT UEs) with a slot of 2 ms. A diagram for the coexistence of LTE and IoT PRBs is depicted in Fig 1. This case is of particular interest since it allows a significant reduction in the complexity of the UE transmitter implementation, and increases the amount of UEs simultaneously connected to the BS. It is important to note that due to the different numerology, there is interference between LTE and IoT UEs, i.e., this scenario is not equivalent to an OFDMA system.

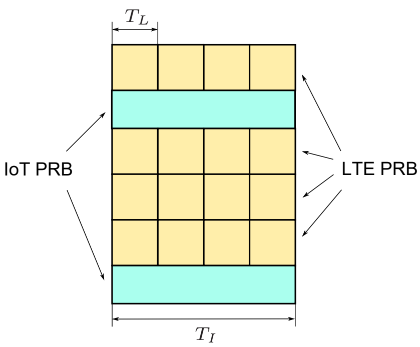

Fig. 1. PRB structure for the coexistence of LTE and IoT in the Uplink.

A block diagram of the IoT UE is shown in Fig. 2. First, the complex base-band symbols are extended to consider the cyclic prefix (CP) N_{cpI} and then are converted to the analog domain. After that, they are modulated in a carrier of frequency $f_c+(k+iM_I)/T_I$, corresponding to the subcarrier k of the i-th PRB, centered at f_c. Without loss of generality, we call UE k to the node allocated to subcarrier k of PRB i. The discrete baseband equivalent of the IoT UE k transmitted signal is

$$x_{k,i,\ell}(n) = X_{k,i,\ell} \exp\left(\frac{j2\pi n}{N_I}(k+iM_I)\right) \quad \text{for } -N_{cpI} \le n \le N_I \tag{1}$$

where $X_{k,i,\ell}$ is the Q-PSK symbol sent by the user k in the block ℓ, N_I is the amount of samples in the IoT symbol, and N_{cpI} the CP.

The LTE signal represents an interference to the PRBs asigned to IoT UEs. Following the block diagram in Fig. 2, the transmitted signal by the LTE UE results

$$v_\ell(n) = \sum_{k=0, k\notin\mathcal{I}_{IoI}}^{N_L-1} V_{k,\ell} \exp\left(\frac{j2\pi kn}{N_L}\right) \quad \text{for } -N_{cpL} \le n \le N_L \tag{2}$$

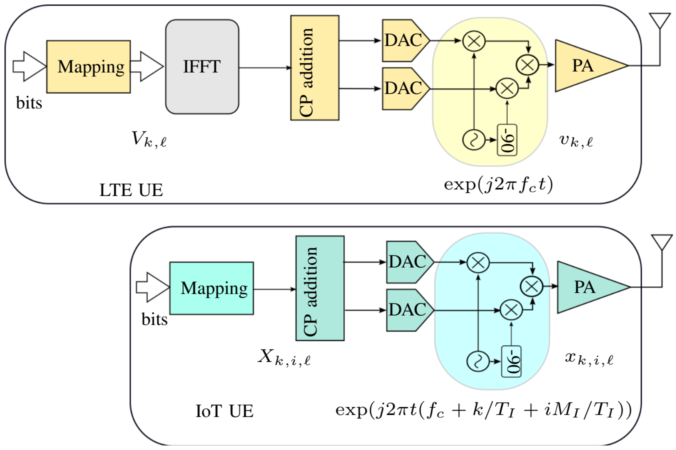

Fig. 2. LTE UE and IoT UE block diagram.

where $V_{k,\ell}$ are M-QAM symbols sent by LTE UEs, $\mathcal{I}_{IoI}$ is the index set of the carriers that are allocated to IoT UEs, $N_L = N_I/4$ is the OFDM symbol length, and N_{cpL} the CP. Note that we do not distinguish among different LTE UEs since we are focused in overall interference they generate.

We define the IoT channel of user k of PRB i as $h_{k,i}(n)$, and the LTE channel as $h_L(n)$. If we consider that the CPs length of LTE and IoT modulations are longer than the channel impulse response, then the received signal at the BS can be expressed as

$$\begin{aligned} y_\ell(n) = &\sum_{i=0, i\notin\mathcal{R}_{IoI}}^{N_{rb}-1} \sum_{k=0}^{M_I-1} H_{k,i}(k+iM_I)X_{k,i,\ell} \\ &\times \exp\left(\frac{j2\pi n}{N_I}(k+iM_I)\right) \\ &+ \sum_{k=0,k\notin\mathcal{I}_{IoI}}^{N_L-1} H_L(k)V_{k,\ell}\exp\left(\frac{j2\pi kn}{N_L}\right) + w(n) \end{aligned} \tag{3}$$

where $\mathcal{R}_{IoI}$ is the index set of PRB allocated to IoT, $N_{rb} = N_L/M_L = N_I/M_I$ is the total amount of PRBs, $H_{k,i}(k)$ is the N_I-length discrete Fourier transforms (DFT) of $h_{k,i}(n)$, $H_L(k)$ is the N_L-length DFT of $h_L(n)$, and $w(n)$ is AWGN.

As the sample rate of both systems is the same ($T_L/N_L = T_I/N_I$), the receiver at the BS can be implemented with a common RF front end. After the downconversion and digitalization, the samples are rearranged to form subframes in each system, according to the amount of samples defined previously (N_{cpL}, N_{cpI}, N_L, and N_I). It is important to note from (3) that the demodulation of IoT is performed by an N_I-FFT, whereas the LTE demodulation by an N_L-FFT. Since the PRBs have different length, there is interference between the systems. A block diagram is presented in Fig. 3.

In the next Section, we describe some possible interference scenarios to study how LTE UEs and hardware imperfections affect the performance of IoT devices.

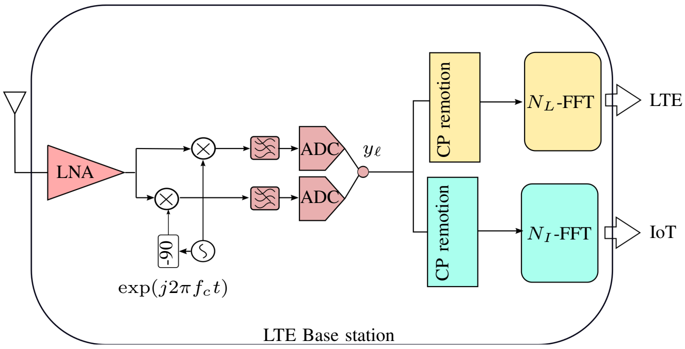

Fig. 3. BS dual demodulation.

III. Interference Scenarios

IoT nodes are usually low power and low cost devices. The power constraint limits the transmitted power, and as a consequence, the interference of IoT over the LTE signal can be neglected. To overcome the power limitation, IoT implements a repetitive code strategy to increase the effective SNR 20dB over LTE specifications [3]. In this work, we focus on the interference of LTE over IoT UEs, since it is of more practical importance [10]. On the other hand, low cost devices are prone to have large RF impairments and synchronization offsets that produce intercarrier and interuser interference, that reduce the system performance. Additionally, both constraints imply that the computation capacity is limited.

As we explained before, the LTE signal is not orthogonal to the IoT. The power leakages from LTE PRBs to those of IoT, following a sinc envelope given by the squared symbol pulse shape in time domain. Then, a simple method to reduce the interference between the systems is to include guard bands between PRBs belonging to LTE and IoT.

In order to allow a large number of simultaneous transmitting IoT UEs, NB-IoT considers a mode with 3.75 kHz of intercarrier spacing. Although this also reduces the implementation complexity, it makes the system more sensitive to RF imperfections related to the oscillator and mixer inaccuracies, such as carrier frequency offset, I/Q imbalance, and phase noise. For frequencies around 2 GHz, as the used in LTE-A networks, oscillators are quite stable and the phase noise does not pose a problem. We consider that the time offset is corrected in the acquisition phase. For this reason, in this work we only consider the CFO and I/Q imbalance. Different to the interference between LTE and IoT, the CFO and I/Q imbalance cause interference between users that belong to the same PRB.

IV. Numerical Results

In this section we evaluate numerically the interference scenarios presented in Section III. First, we show the effectivity of guard bands in the IoT PRB to mitigate the interference of the LTE signal. Then, we analyze the intra-PRB interference of IoT UEs due to CFO and I/Q imbalance.

TABLE I
Summary of System Parameters

Parameter	LTE	IoT
Subcarriers	$N_L = 1024$	$N_I = 4096$
CP	$N_{cpL} = 16$	$N_{cpI} = 64$
PRB size	$M_L = 12$	$M_I = 48$
Inter. spacing	$1/T_L$ =15 kHz	$1/T_I$ =3.75 kHz
Constellation	64-QAM	Q-PSK

We consider the uplink of a system where LTE and IoT UEs coexist. System parameters are defined in Table I. Each carrier in the IoT PRB belong to a different user with its own hardware and synchronization imperfections. In the simulation we consider only an IoT PRB, since it is the worst interference case.

In the Fig. 4, we show the averaged BER of IoT UEs that belong to the PRB, under the interference of LTE UEs that fully complete the rest of the PRBs. The figure evaluates the effect of different guard bands in the mitigation of the LTE interference. The guard bands are allocated at the edge of the IoT PRB. Both signals have the same received power. From the figure, it is evident that even large guard bands do not get a reasonable BER performance. This is a consequence of the slow decay of the sinc function. We conclude that a more sophisticated technique is needed in the BS to compensate for the LTE interference, in order to get a better performance without sacrificing bandwidth.

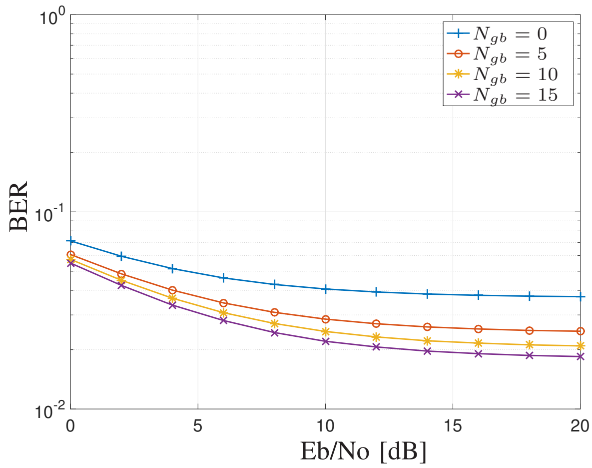

Fig. 4. Averaged BER of the IoT UEs under LTE interference. Effect of guard bands at the edge of the IoT PRB.

To evaluate the BER degradation due to the CFO, we consider a single IoT UE without active LTE UEs. In Fig. 5, we plot the average BER of IoT users for different CFO ranges. The CFO is normalized to the intercarrier spacing, different for each user, and uniformly distributed in the range $\{-\epsilon_L, \epsilon_L\}$. In the curve we see that the average BER of UEs in the IoT PRB is adequate for CFO values below 0.1. This only can be achieved for static applications and if the IoT UE synchronizes with the BS in the downlink, prior to the uplink transmission.

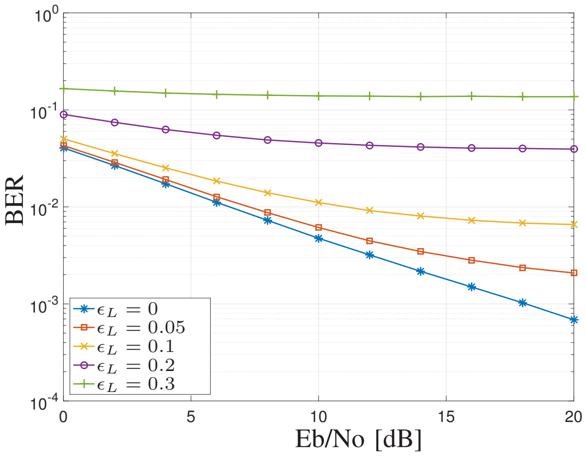

Fig. 5. Averaged BER of the IoT UEs due to CFO. No active LTE users.

Finally, the degradation in the averaged BER due to I/Q imbalance is shown in Fig. 6. The parameters α and θ are respectively the amplitude and phase mismatches of the mixer. As we observe from the figure, the I/Q imbalance does not cause a noticeable performance drop due to the low constellation used by IoT devices.

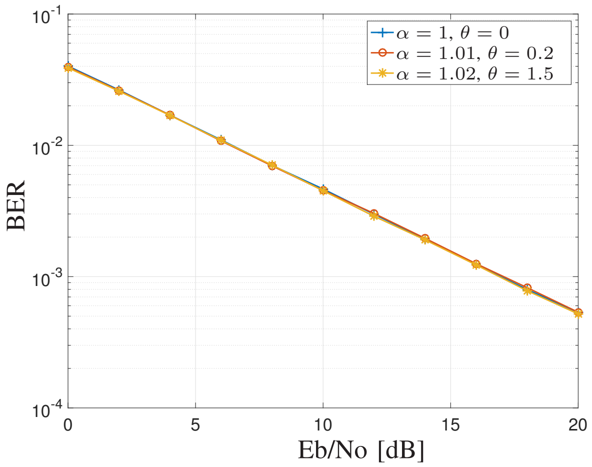

Fig. 6. Averaged BER of the IoT UEs due to I/Q imbalance. No active LTE users.

V. Conclusion

In this paper we analyze the feasibility of the coexistence of LTE and internet-of-things (IoT) user equipements (UE)s, for the uplink multiple access. We consider the IoT single tone protocol with 3.75 kHz intercarrier spacing, that allows several UEs to share a single physical resource block (PRB), with a fraction of the implementation complexity. The coexistence with LTE introduces interference in the IoT receiver, and the reduction of the intercarrier spacing makes the system less robust to carrier frequency offset (CFO) and the I/Q imbalance. We show that the LTE signal introduces a strong interference in the IoT receiver. The addition of guard bands at the edges of the IoT PRB does not provide the necessary isolation level and the performance of the system is compromised. On the other hand, we show that the IoT receiver is robust to CFO levels below 0.1 and that the I/Q imbalance does not produce a noticeable drop in the performance.

References

[1] D. Giusto, A. Iera, G. Morabito, and L. Atzori, *The Internet of Things*. Springer, 2010.

[2] G. A. Akpakwu, B. J. Silva, G. P. Hancke, and A. M. Abu-Mahfouz, “A survey on 5G networks for the internet of things: Communication technologies and challenges,” *IEEE Access*, vol. 6, pp. 3619–3647, 2018.

[3] Y. P. E. Wang, X. Lin, A. Adhikary, A. Grovlen, Y. Sui, Y. Blankenship, J. Bergman, and H. S. Razaghi, “A primer on 3GPP narrowband internet of things,” *IEEE Communications Magazine*, vol. 55, no. 3, pp. 117–123, March 2017.

[4] M. R. Palattella, M. Dohler, A. Grieco, G. Rizzo, J. Torsner, T. Engel, and L. Ladid, “Internet of things in the 5G era: Enablers, architecture, and business models,” *IEEE Journal on Selected Areas in Communications*, vol. 34, no. 3, pp. 510–527, March 2016.

[5] H. Malik, H. Pervaiz, M. M. Alam, Y. L. Moullec, A. Kuusik, and M. A. Imran, “Radio resource management scheme in NB-IoT systems,” *IEEE Access*, vol. 6, pp. 15 051–15 064, 2018.

[6] A. Ijaz, L. Zhang, M. Grau, A. Mohamed, S. Vural, A. U. Quddus, M. A. Imran, C. H. Foh, and R. Tafazolli, “Enabling massive IoT in 5G and beyond systems: PHY radio frame design considerations,” *IEEE Access*, vol. 4, pp. 3322–3339, 2016.

[7] S. Shin, “NB-IoT system modeling: Simple doesnt mean easy,” *Keysight Technologies: White paper*, 2016.

[8] “3rd generation partnership project; technical specification group radio access network; evolved universal terrestrial radio access (E-UTRA); NB-IoT; technical report for (BS) and (UE) radio transmission and reception (release 13),” *3GPP TR 36.802 V13.0.0*, 2016.

[9] L. Zhang, A. Ijaz, P. Xiao, and R. Tafazolli, “Channel equalization and interference analysis for uplink narrowband internet of things (NB-IoT),” *IEEE Communications Letters*, vol. 21, no. 10, pp. 2206–2209, Oct 2017.

[10] “3rd generation partnership project; discussion on multiplex of uplink signal with different subcarrier spacing,” *3GPP TSG RAN WG1 Meeting 84*, Feb 2016.